# Ignition Criterion for General Kinetics in a Catalytic Monolith

**Karthik Ramanathan and Vemuri Balakotaiah**
Dept. of Chemical Engineering, University of Houston, Houston, TX 77204

**David H. West**
The Dow Chemical Company, Freeport, TX 77541

*DOI 10.1002/aic.10757*
*Published online December 30, 2005 in Wiley InterScience (www.interscience.wiley.com).*

*Keywords: catalytic monolith, light-off, ignition, carbon monoxide oxidation, nonuniform catalyst distribution*

## Introduction

Monolithic catalytic reactors are used in a variety of environmental and industrial applications. The most common is its use in the control of automobile emissions. Other applications include oxidation of volatile organic compounds, catalytically stabilized thermal burners, catalytic partial oxidation of hydrocarbons, and removal of $NO_x$ from power plant and furnace exhaust gases. The monolith reactor is a continuous unitary structure with a large number of small, long channels (diameter 0.5–2 mm; length 5–20 cm) in parallel, through which the reacting fluid flows. These channels can be of any cross-sectional shape including circular, square, triangular, hexagonal, or sinusoidal. The catalyst (containing the precious metals such as Pt, Pd, and Rh) is deposited on the walls of the monolith channels as a porous washcoat. Because of the small channel dimensions, the flow is laminar in most cases with Reynolds numbers in the range 100 to 1000. The reactants in the fluid phase are transported to the surface of the catalyst and within the catalyst by diffusion and in the axial direction mainly by convection.

There is extensive literature dealing with experimental, modeling, and simulation results of catalytic monoliths. Review articles by Cybulski and Moulijn,[1] Lox and Engler,[2] and Groppi et al.,[3] and books by Becker and Pereira[4] and Hayes and Kolaczkowski[5] summarize the recent progress. The light-off (or ignition) in catalytic monoliths has also been studied by several researchers. Please et al.,[6] Leighton and Chang,[7] and Keith et al.[8] analyzed the propagation of the ignition front. Oh and Cavendish[9] studied the catalytic converter light-off using packed-bed and monolith reactor models. The light-off behavior of the monolithic reactor depends not only on the design variables such as the channel dimensions, support and washcoat properties, and catalyst loading but also on the operating variables such as the inlet gas velocity, composition, and temperature. We recently presented an explicit light-off criterion for a monolithic reactor for the case of a first-order reaction.[10-12] The advantage of such an explicit algebraic criterion is that the dependency of the light-off behavior on various design and operating variables can be determined for any given kinetics, without the extensive numerical calculations using the full two-phase or more complex models. The purpose of this work is to extend our earlier light-off criterion for a first-order reaction to more general kinetics. We also use the example of carbon monoxide oxidation to illustrate the new and general light-off criterion.

## Mathematical Model

The one-dimensional, two-phase steady-state model considered here is the same as that presented by Ramanathan et al.[10] and may be written as the following system of equations:

$$\bar{u}\,\frac{\partial C_m}{\partial x} = -\frac{k_c(x)}{R_\Omega}\,(C_m - C_s) \tag{1}$$

$$\bar{u}\rho_f c_{p_f}\,\frac{\partial T_f}{\partial x} = -\frac{h(x)}{R_\Omega}\,(T_f - T_s) \tag{2}$$

$$k_c(x)(C_m - C_s) = a_c(x)\,R_v(C_s, T_s)\,\delta_c\eta \tag{3}$$

$$\delta_w k_w\,\frac{\partial^2 T_s}{\partial x^2} + a_c(x)\,\delta_c(-\Delta H_R)\,R_v(C_s, T_s)\eta - h(x)(T_s - T_f) = 0 \tag{4}$$

Correspondence concerning this article should be addressed to V. Balakotaiah at bala@uh.edu.

$$D_e \frac{\partial^2 C}{\partial y^2} = a_c(x) R_v(C, T_s) \qquad 0 < y < \delta_c \tag{5}$$

$$C = C_s \ @ \ y = 0 \qquad \frac{\partial C}{\partial y} = 0 \ @ \ y = \delta_c \tag{6}$$

$$\eta \delta_c a_c(x) R_v(C_s, T_s) = -D_e \left.\frac{\partial C}{\partial y}\right|_{y=0} \tag{7}$$

$$C_m = C_{m,in} \ @ \ x = 0 \tag{8}$$

$$T_f = T_{f,in} \ @ \ x = 0 \tag{9}$$

$$\frac{\partial T_s}{\partial x} = 0 \ @ \ x = 0, L \tag{10}$$

The fluid- and solid-phase species and energy balances are given by Eqs. 1–4. Equations 5 and 6 describe the reactant concentration profile in the washcoat, whereas Eq. 7 gives the washcoat effectiveness factor ($\eta$) for the reaction. Equations 8–10 define the boundary conditions. Here, $x$ and $y$ represent the axial coordinate along the channel and depth into the washcoat (from the fluid–washcoat interface), respectively. $T_f$ and $C_m$ represent the cup-mixing temperature and concentration of the reactant, in the fluid phase, whereas $T_s$ and $C_s$ denote the solid-phase temperature and the reactant concentration at the fluid–solid interface. $a_c(x)$ is the normalized activity (catalyst distribution) profile along the channel [$(1/L)\int_0^L a_c(x)dx = 1$] and $R_v(C, T)$ is the intrinsic reaction rate based on washcoat volume [$R_v(C, T)$ has units of moles per unit washcoat volume per unit time]. More details about the model and explanation of the other terms in the above equations can be found in the Notation and in Ramanathan et al.[10-12]

Here, $h(x)$ and $k_c(x)$ represent the heat- and mass-transfer coefficients along the channel, respectively. The above model is valid for any arbitrary channel shape and washcoat profile, provided $\delta_c \ll R_\Omega$. (In practice, this condition is satisfied because $\delta_c$ is around 10 to 50 $\mu$m, whereas $R_\Omega$ is around 200 to 500 $\mu$m.) The values of the heat- and mass-transfer coefficients, expressed as Nusselt (Nu)/Sherwood (Sh) numbers for various geometries can be found in Ramanathan et al.[12]

## Light-off (Ignition) Criterion for General Kinetics

By ignition or light-off we imply that the steady-state (bifurcation) diagram of solid exit temperature $T_s(L)$ (or fluid-phase exit conversion or temperature) vs. the inlet fluid temperature $T_{f,in}$ (or residence time) is an S-shaped diagram with the ignition point in the feasible region. Thus, when our light-off criterion is satisfied, the monolith will attain the ignited steady state. According to our definition, the boundary between light-off and no light-off is determined by the *hysteresis locus* [the appearance of an ignition and an extinction point in the bifurcation diagram of $T_s(L)$ vs. $T_{f,in}$]. In this work, we assume that the parameters are such that ignition occurs in the monolith. The ignition/light-off criterion for the case of a single first-order reaction in a catalytic monolith with uniform catalyst loading [$a_c(x) = 1$] was presented in Ramanathan et al.[10] This criterion was extended to the case of nonuniform catalyst loading and was presented in Ramanathan et al.[12]

Now we extend this criterion to the case of a single reaction with general kinetics. We make the following assumptions in deriving the light-off criterion:

(1) consumption of reactant is neglected (which is justified before ignition)
(2) negligible diffusional resistance in the washcoat ($\eta = 1$) before ignition
(3) conduction in the solid phase is negligible [or equivalently, the Peclet number, $\mathrm{Pe}_h = \bar{u}L\rho_f c_{p_f} R_\Omega/(k_w \delta_w) \gg 1$]
(4) the ratio of transverse diffusion time ($R_\Omega^2/D_m$) to the convection time ($L/\bar{u}$) is small and thus the position dependency of the transfer coefficients can be neglected [$\mathrm{Nu}(x) = \mathrm{Nu}_{H_1,\infty}/4$ and $\mathrm{Sh}(x) = \mathrm{Sh}_{H_1,\infty}/4$]
(5) uniform catalyst loading [$a_c(x) = 1$]

With the above-mentioned assumptions and approximations, the solid- and the fluid-phase energy balances can be simplified as

$$\delta_c(-\Delta H_R) R_v(C_{m,in}, T_s) = h_{H1,\infty}(T_s - T_f) \tag{11}$$

$$\bar{u}\rho_f c_{p_f} \frac{\partial T_f}{\partial x} = -h_{H_1,\infty}(T_f - T_s)/R_\Omega \tag{12}$$

The above equations represent the two-phase plug flow model. Here, $h_{H_1,\infty}$ represents the asymptotic value of the heat transfer coefficient and is equal to $\mathrm{Nu}_{H_1,\infty}\mathrm{k_f}/4R_\Omega$. The ignition (light-off) point of this two-phase plug flow model with uniform catalyst loading is obtained by setting the derivative of Eq. 11 with respect to $T_s$ to zero:

$$\delta_c(-\Delta H_R) \frac{d}{dT_s}[R_v(C_{m,in}, T_s)] = h_{H_1,\infty} \tag{13}$$

By solving the above equation we can obtain the solid temperature ($T_{s,ig}$) corresponding to the ignition point. Now, we can determine the location of ignition by integrating Eq. 12 from $T_{s,in}$ to $T_{s,ig}$, which is given by

$$x_{ig} = \frac{\bar{u}\rho_f c_{p_f} R_\Omega}{(-\Delta H_R)\delta_c} \int_{T_{s,in}}^{T_{s,ig}} \frac{\left[1 - \dfrac{(-\Delta H_R)\delta_c}{h_{H_1,\infty}} \dfrac{d}{dT_s}[R_v(C_{m,in}, T_s)]\right]}{R_v(C_{m,in}, T_s)} dT_s$$

$$= \frac{\bar{u}\rho_f c_{p_f} R_\Omega}{(-\Delta H_R)\delta_c} \left\{ \int_{T_{s,in}}^{T_{s,ig}} \frac{dT_s}{R_v(C_{m,in}, T_s)} - \frac{(-\Delta H_R)\delta_c}{h_{H_1,\infty}} \ln\left[\frac{R_v(C_{m,in}, T_{s,ig})}{R_v(C_{m,in}, T_{s,in})}\right] \right\} \tag{14}$$

In the above expression, $T_{s,in}$ represents the solid temperature at the inlet of the reactor and is obtained by solving the following algebraic equation:

$$\delta_c(-\Delta H_R) R_v(C_{m,in}, T_{s,in}) = h_{H_1,\infty}(T_{s,in} - T_{f,in}) \tag{15}$$

If the location of ignition is less than the channel length (that is, $x_{ig} < L$), we have ignition in the monolith. Thus, the ignition criterion may be written as

$$\frac{(-\Delta H_R)\delta_c L}{\bar{u}\rho_f c_{p_f} R_\Omega} > \left( \int_{T_{s,in}}^{T_{s,ig}} \frac{dT_s}{R_v(C_{m,in}, T_s)} - \frac{(-\Delta H_R)\delta_c}{h_{H_1,\infty}} \ln\left[\frac{R_v(C_{m,in}, T_{s,ig})}{R_v(C_{m,in}, T_{s,in})}\right] \right) \quad (16)$$

If the location of ignition is close to the inlet we have a front-end ignition ($x_{ig} \simeq 0$). Front-end ignition basically means that Eq. 11 starts having multiple solutions at the inlet (that is, $T_f = T_{f,in}$). It should be noted that the above expression for finding the location of ignition in a monolith channel (with zero solid conduction) is valid for a single reaction with arbitrary kinetics.

When the slope of the heat generation curve at the ignition temperature is greater than that of the heat removal curve (at the inlet), then we have a front-end ignition and we could express the criterion for front-end ignition as

$$\frac{\delta_c(-\Delta H_R) R_v(C_{m,in}, T_{s,ig})}{h_{H_1,\infty}(T_{s,ig} - T_{f,in})} > 1 \quad (17)$$

Instead of expressing Eqs. 16 and 17 in terms of the reaction rate at the ignition temperature, we could rewrite them (by expressing the reaction rate at the inlet fluid temperature, $T_{f,in}$) as

$$\frac{(-\Delta H_R)\delta_c LER_v(C_{m,in}, T_{f,in})}{\bar{u}\rho_f c_{p_f} R_\Omega R_g T_{f,in}^2} > \frac{ER_v(C_{m,in}, T_{f,in})}{R_g T_{f,in}^2} \left( \int_{T_{s,in}}^{T_{s,ig}} \frac{dT_s}{R_v(C_{m,in}, T_s)} - \frac{(-\Delta H_R)\delta_c}{h_{H_1,\infty}} \ln\left[\frac{R_v(C_{m,in}, T_{s,ig})}{R_v(C_{m,in}, T_{s,in})}\right] \right) \quad (18)$$

$$\frac{(-\Delta H_R)\delta_c eER_v(C_{m,in}, T_{f,in})}{h_{H_1,\infty} R_g T_{f,in}^2} > \frac{R_v(C_{m,in}, T_{f,in})}{R_v(C_{m,in}, T_{s,ig})} \frac{eE(T_{s,ig} - T_{f,in})}{R_g T_{f,in}^2} \quad (19)$$

A plot of the right-hand side (rhs) of Eqs. 18 and 19 for various values of $T_{f,in}$ yields interesting results. We note that these expressions vary from 1 to 0 and 0 to 1, respectively, as we increase $T_{f,in}$ from a low value (say 300 K) to the value of $T_{f,in}$ at which front-end ignition is favored. We shall designate the rhs of Eqs. 18 and 19 as Term1 and Term2, respectively. Adding the above two equations and plotting the rhs of the resulting equation (Term1 + Term2) with $T_{f,in}$ shows that the rhs is close to unity for the entire range of $T_{f,in}$. Thus, we can approximate the ignition criterion as

$$\frac{(-\Delta H_R)\delta_c LER_v(C_{m,in}, T_{f,in})}{\bar{u}\rho_f c_{p_f} R_\Omega R_g T_{f,in}^2} + \frac{(-\Delta H_R)\delta_c eER_v(C_{m,in}, T_{f,in}) 4R_\Omega}{\mathrm{Nu}_{H_1,\infty} k_f R_g T_{f,in}^2} > 1 \quad (20)$$

We note that this criterion involves only the overall kinetic expression and various geometrical, transport, and kinetic parameters. If the above criterion is satisfied there is ignition in the monolith and the location of ignition is given by Eq. 14. If the second term in the above equation exceeds unity, then there is front-end ignition and the condition for this front-end ignition can be expressed as

$$\frac{(-\Delta H_R)\delta_c eER_v(C_{m,in}, T_{f,in}) 4R_\Omega}{\mathrm{Nu}_{H_1,\infty} k_f R_g T_{f,in}^2} > 1 \quad (21)$$

In Eq. 20, the first term represents ignition at the reactor scale and the second term represents local or front-end ignition. Depending on the magnitude of the terms, we could determine the nature of ignition in the monolith. When the second term exceeds unity, then we have a front-end ignition. If the first term exceeds unity and the second term is negligible compared to unity we have back-end ignition. We could also predict the location of ignition using Eq. 14. When the ignition criterion is barely satisfied and the magnitude of both the terms is less than unity, it is always a back-end ignition.

It has been shown that nonuniform catalyst loading along the channel length could be used to favor front-end ignition.[12] The preceding results could be extended to the case of nonuniform catalyst loading. The final result is the light-off criterion

$$\frac{(-\Delta H_R)\delta_c LER_v(C_{m,in}, T_{f,in})}{\bar{u}\rho_f c_{p_f} R_\Omega R_g T_{f,in}^2} + \frac{\max[a_c(x)](-\Delta H_R)\delta_c eER_v(C_{m,in}, T_{f,in}) 4R_\Omega}{\mathrm{Nu}_{H_1,\infty} k_f R_g T_{f,in}^2} > 1 \quad (22)$$

For the case of negligible washcoat diffusional resistance, the catalyst distribution does not affect the ignition at the reactor scale (the first term in the above equation). The catalyst distribution affects only the local ignition behavior and if the second term in the above equation is greater than unity, then the ignition occurs at the location where $a_c(x)$ is maximum. Given that, for most cases, nonuniform catalyst distribution is used to favor local ignition, the location of ignition for these cases will be the location where $a_c(x)$ is maximum and a separate expression for the location of ignition is not needed. The criterion for front-end ignition with nonuniform catalyst loading can be expressed as

$$\frac{a_c(0)(-\Delta H_R)\delta_c eER_v(C_{m,in}, T_{f,in}) 4R_\Omega}{\mathrm{Nu}_{H_1,\infty} k_f R_g T_{f,in}^2} > 1 \quad (23)$$

where $a_c(0)$ represents the magnitude of the catalyst distribution at the inlet.

It should be pointed out that the above explicit ignition criteria (Eqs. 22 and 23) have been derived for the case where reaction activation energy is much greater than the desorption activation energy, that is, the variation of $R_v(C, T)$ with $T$ is

closer to an Arrhenius expression. (Adsorption activation energy is very small for most practical cases.) When the desorption activation energy is less than 5 times the reaction activation energy, the ignition criterion predicts the ignition temperature within 5 K. If this is not the case, accurate prediction of ignition involves numerical solution of Eq. 15 and using $x_{ig}$ calculated from Eq. 14. These expressions were derived without the above approximation (of reaction activation energy being much larger than the desorption energy).

For the case of infinite solid conduction, the approximate ignition criterion for the case of a single reaction with general kinetics can be written as

$$\frac{(-\Delta H_R) R_v(C_{m,in}, T_{f,in}) E_1 e \delta_c L}{\bar{u}\rho_f c_{p_f} R_\Omega R_g T_{f,in}^2} > 1 \tag{24}$$

and is obtained by using the simplified model equations for infinite solid conduction. (The solid-phase energy balance for this case is an algebraic equation.) It should be noted that, because the solid temperature is uniform in the monolith, ignition occurs uniformly along the channel length. It can be easily shown that the difference in the solid temperature required for ignition for zero solid conduction (front-end ignition) and infinite solid conduction is

$$T_{s,ig}|_{k_w \to 0} - T_{s,ig}|_{k_w \to \infty} \approx \frac{R_g T_{f,in}^2}{E} \ln\left(\frac{\mathrm{Nu}_{H_1,\infty} k_f L}{4\bar{u}\rho_f c_{p_f} R_\Omega^2}\right)$$

and for typical values of reactor parameters, this difference is about 55 to 60 K. In other words, the inlet fluid temperature required for ignition in a monolith with higher solid conduction will be less compared to a monolith with very low solid conduction. This again emphasizes that for steady-state operation (where ignition is required in the monolith), high solid conduction is preferred. For transient operation, however, a monolith with high solid conduction takes considerable time to reach the ignition temperature because the entire monolith has to be heated to the ignition temperature. In most cases, a monolith with low solid conduction is preferred when transient operation is involved because a local ignition (front-end) can be favored easily and the transient time would be small. The contrasting effects of low and high solid conduction have been illustrated in detail elsewhere.[10-12]

A comparison between the first term of the ignition criterion for the single reaction with zero solid conduction (Eq. 22), with the ignition criterion with infinite solid conduction (Eq. 24), reveals that the only difference is the appearance of the factor ($e$) in these terms. It was shown by Balakotaiah[13] that the factor in the first term changes from 1 (for zero conduction or the plug flow limit) to $e = 2.718$ (for infinite conduction or the CSTR limit). For intermediate values of solid conduction, this factor can be expressed analytically as

$$g(\mathrm{Pe}_h) = \frac{1}{(\sigma_\theta^2)^{\sigma_\theta^2/(1-\sigma_\theta^2)}} \qquad \sigma_\theta^2 = \frac{2}{\mathrm{Pe}_h} - \frac{2}{\mathrm{Pe}_h^2}(1 - e^{-\mathrm{Pe}_h}) \tag{25}$$

where $\mathrm{Pe}_h = \bar{u}L\rho_f c_{p_f} R_\Omega/(k_w \delta_w)$ represents the axial heat Peclet number. The second term in the ignition criterion, Eq. 22, represents local or front-end ignition and is not affected by finite conduction in the solid. Combining the case of zero and infinite solid conduction, the ignition criterion for a single reaction with finite solid conduction can be written as

$$\frac{(-\Delta H_R)\delta_c L E R_v(C_{m,in}, T_{f,in})\, g(\mathrm{Pe}_h)}{\bar{u}\rho_f c_{p_f} R_\Omega R_g T_{f,in}^2} + \frac{\max[a_c(x)](-\Delta H_R)\delta_c e E R_v(C_{m,in}, T_{f,in}) 4R_\Omega}{\mathrm{Nu}_{H_1,\infty} k_f R_g T_{f,in}^2} > 1 \tag{26}$$

It should be mentioned that the solid conduction does not affect front-end ignition.[10]

In short, Eq. 26 represents the ignition criterion for a single reaction with general kinetics and finite solid conduction. If the first term is greater than unity (with the second term negligible), then we have a back-end ignition. When the second term exceeds unity (with the first term negligible compared to the second term), then the ignition occurs at the location where the catalyst distribution function $a_c(x)$ is maximum. If the maximum of $a_c(x)$ occurs at $x = 0$ (that is, at the inlet), then we have a front-end ignition. For very low solid conduction and uniform catalyst distribution, we could find the location of ignition using Eq. 14. When the solid conduction is very high, the ignition criterion is given by Eq. 24 and ignition is uniform.

## Analysis of Light-off Behavior of CO Oxidation Using the Ignition Criterion

The results obtained above can be used to analyze the influence of the various design and operating variables on the light-off behavior and location of light-off in a catalytic monolith. With the help of these results, we could also find minimum inlet temperature required for light-off and its sensitivity to various other design and operating variables. We also compare the approximate local ignition criterion (Eq. 21) with the more accurate local ignition criterion (Eq. 17) using carbon monoxide oxidation (which has Langmuir–Hinshelwood kinetics) as an example. The effect of washcoat diffusion is assumed to be negligible before ignition. For typical parameter values (close to ignition), the effectiveness factor is around unity (as will be shown later) and thus for practical purposes it can be assumed to be equal to unity. After ignition, however, washcoat diffusion effects are significant and cannot be neglected.

The kinetics of carbon monoxide oxidation, as given by Voltz et al.,[14] is expressed as

$$R_v = \frac{2.68 \times 10^{18} \exp\left(-\dfrac{12556}{T}\right) y_{co} y_{o_2}}{T\left[1 + 65.5 \exp\left(\dfrac{961}{T}\right) y_{co}\right]^2} \qquad \mathrm{mol\ m^{-3}\ s^{-1}} \tag{27}$$

where $y_{co}$ and $y_{o_2}$ represent the mole fractions of CO and $O_2$, respectively. We assume that the oxygen concentration is in excess and remains constant at 5% (mole fraction). Figure 1 shows the plot of Term1, Term2, and Term1 + Term2 as a function of $T_{f,in}$ for three different CO inlet concentrations. The parameters used are listed in Table 1. In the table, $C_o$ represents

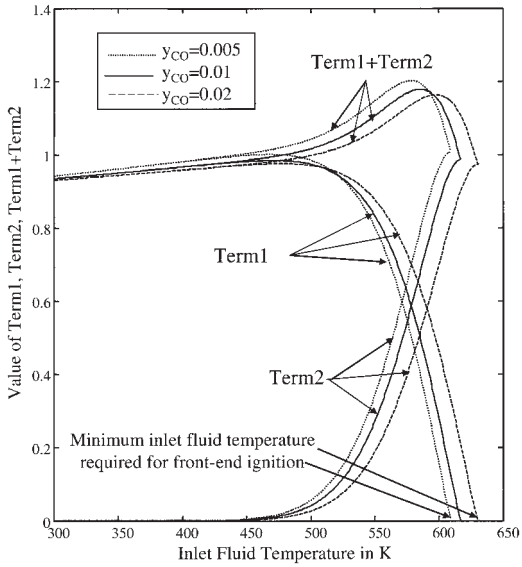


**Figure 1. Plots of Term1, Term2, and Term1 + Term2 as a function of the inlet fluid temperature for the case of carbon monoxide oxidation.**

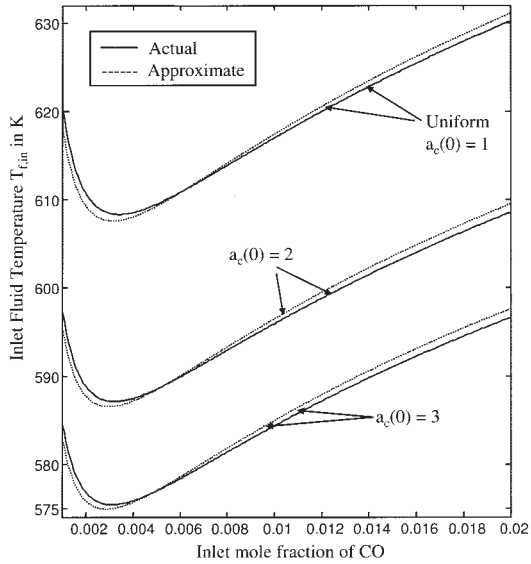


**Figure 2. Minimum inlet fluid temperature required for front-end ignition for the case of carbon monoxide oxidation with uniform and nonuniform catalyst loading.**

the total gas-phase concentration ($C_{co} = y_{co}C_o$). For CO oxidation, the sum Term1 + Term2 varies between 0.92 and 1.23 for all values of $T_{f,in}$ and thus we could use Eq. 20 to verify whether we will have ignition in the monolith. For inlet fluid temperature values $>$ 617 K (for $y_{co} = 0.01$) and 630 K (for $y_{co} = 0.02$), there is front-end ignition in the monolith and Term1 goes to zero and Term2 is approximately unity.

We compare the boundary between front-end light-off and no front-end light-off using the approximated front-end ignition criterion (Eq. 21) and the actual criterion (Eq. 17) for the case of uniform catalyst distribution. Note that before ignition, the effectiveness factor is close to unity and we find that it varies between 0.9 and 1.0 (before ignition) for most practical cases. The top curve in Figure 2 shows the minimum inlet fluid temperature required for front-end ignition as a function of the inlet CO mole fraction. As can be seen, the approximate criterion compares well with the actual one (within 2–3 K). It is interesting to note that there exists a critical mole fraction of CO for which the inlet fluid temperature required for ignition is a minimum. For a mole fraction lower or higher than this critical value ($y_{co} \approx 0.003$), the inlet fluid temperature required for ignition increases. This is because of the nonmonotonic nature of the CO kinetics. For very low concentration values, the Langmuir–Hinshelwood kinetics behaves like a positive-order kinetics and for higher values of concentration, the negative-order contribution is more pronounced. (Note that for monotone kinetics, as we continue to increase the inlet concentration the minimum inlet fluid temperature required for ignition continues to decrease.) For the parameters chosen, the mole fraction of CO is around 0.003 and front-end ignition is favored at a much lower temperature (around 607 K). In Figure 2, we also show similar plots for the case of nonuniform catalyst loading with more catalyst near the inlet. The interesting result here is that the minimum inlet fluid temperature for ignition is reduced by 20 K when we distribute such that the amount of catalyst near the inlet is twice as high [$a_c(0) = 2$] and is reduced by 30 K when $a_c(0) = 3$.

**Table 1. Standard Parameter Values for CO Oxidation**

| | | | |
|---|---|---|---|
| $\bar{u}$ | 5 m/s | $k_f$ | 0.055 W m$^{-1}$ K$^{-1}$ |
| $R_\Omega$ | 0.5 mm | $k_w$ | 0.8304 W m$^{-1}$ K$^{-1}$ |
| $\delta_w$ | 175 $\mu$m | $y_{o_2}$ | 0.05 |
| $\delta_c$ | 25 $\mu$m | $(-\Delta H_R)$ | $2.83 \times 10^5$ J/mol |
| $c_{p_f}$ | $1.089 \times 10^3$ J kg$^{-1}$ K$^{-1}$ | $D_e$ | $8 \times 10^{-6}$ m$^2$/s |
| $\rho_w$ | 2500 kg/m$^3$ | $D_m$ | $8.82 \times 10^{-5}$ m$^2$/s |
| $c_{p_w}$ | $1.38 \times 10^3$ J kg$^{-1}$ K$^{-1}$ | $L$ | 0.1 m |
| $\rho_f$ | 0.58 kg/m$^3$ | $T_{s0}$ | 300 K |
| $C_o$ | 20 mol/m$^3$ | $y_{co,in}$ | 0.02 |
| Pe$_h$ | 1086.6 | P | 0.14 |
| Circular geometry | | Nu$_{H_1,\infty}$ | 4.364 |

The location of ignition in the reactor (obtained by Eq. 14) as a function of the inlet fluid temperature for three different inlet concentrations of CO is shown in Figure 3. As the inlet fluid temperature continues to increase, the ignition behavior changes from back-end to front-end ignition. For example, for inlet fluid temperature $<$ 587 K a reactor of length 0.1 m with $y_{co} = 0.02$ does not have ignition and as the inlet fluid temperature continues to increase from 587 to 630 K, the ignition behavior changes from back-end to front-end ignition. This figure also illustrates the nonmonotonic behavior of the inlet mole fraction of CO. As the mole fraction of CO is increased from a low value, the ignition starts to occur at lower temperatures (or shorter channel lengths). However, after a critical value of the mole fraction is reached any increase in the mole fraction delays ignition (higher temperatures or longer channel lengths).

Until ignition, it has been assumed that the washcoat diffusion effects are negligible. Figure 4 shows the variation of the effectiveness factor over a wide range of solid temperature and solid/fluid surface mole fraction. The effectiveness factor is obtained by solving only the (isothermal) diffusion–reaction equation (Eqs. 5–7) in the washcoat for different values of the

solid temperature $T_s$ and surface mole fraction $y_s$ with all other parameter values listed in Table 1. For very low solid temperatures (<600 K), the effectiveness factor is unity. For the chosen parameters, the effectiveness factor reaches a maximum of 1.5 for a solid/washcoat temperature of 740 K and a surface mole fraction of 0.02. For very low surface mole fraction, as the temperature increases the effectiveness factor continues to decrease, which because for low mole fraction values, the CO oxidation kinetics has a positive order. However, for higher surface mole fraction, the effectiveness factor goes above unity for a range of washcoat temperature values and at high temperatures starts to decrease again. This is because the kinetics is nonmonotonic and changes from positive order to negative order and back to positive order. This figure illustrates that the effect of washcoat diffusion before ignition is negligible because the ignition temperatures are typically around 600–650 K.

From the above analysis and results, it is clear that as we change the inlet fluid temperature, the ignition behavior (or the location of ignition) changes from no-ignition to back-end ignition to middle ignition to front-end ignition. A bifurcation diagram of the exit solid temperature vs. the inlet fluid temperature illustrates this in more detail. Depending on the region in the parameter space, the bifurcation diagram can have multiple solutions or a unique solution for the entire range of inlet fluid temperatures. Note that when there is only a unique solution there is no ignition in the monolith. Figure 5 shows a computed bifurcation diagram for the case of wall reaction ($\eta = 1$, negligible washcoat diffusional resistance) for a typical set of parameters. (The bottom diagram shows the solid and fluid mole fractions.) For very low values of the inlet fluid temperature ($T_{f,in}$), the (exit) solid temperature is equal to the inlet fluid temperature and reactant conversion is small (point O in Figure 5). As the inlet fluid temperature is increased from this very low value, the exit solid temperature also continues to

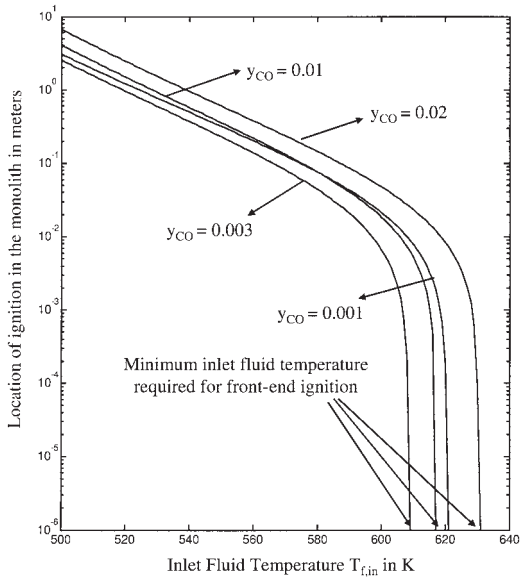


**Figure 3. Location of ignition in the monolith channel as a function of the inlet fluid temperature for the case of carbon monoxide oxidation for uniform catalyst loading.**

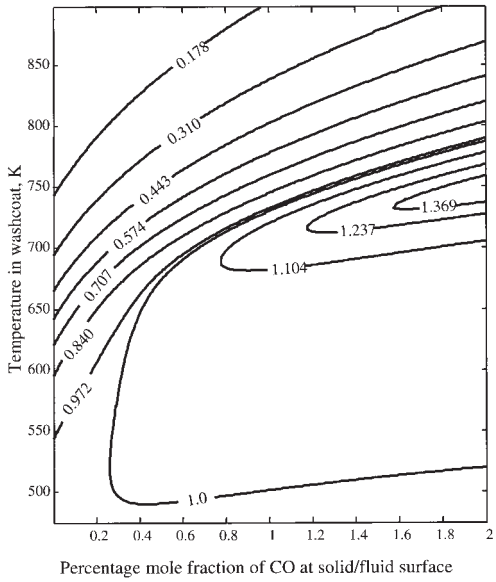


**Figure 4. Effectiveness factor variation with washcoat temperature and surface mole fraction for CO oxidation and for parameter values listed in Table 1.**

increase until it reaches the ignition temperature. The ignition point is represented by point I in the figure and the entire branch OI is the extinguished branch. A small increase above the ignition temperature leads to a substantial increase in the solid temperature and the upper branch or the ignited branch in the bifurcation diagram is reached. A further increase in the inlet fluid temperature increases the exit solid temperature. This branch is represented by AC in the figure. As the inlet fluid temperature continues to decrease from a very high value (in the ignited branch), it reaches the extinction temperature and the extinction point is represented by the point E in the figure. In short, as we increase and later decrease the inlet fluid temperature, the exit solid temperature follows OIAC and CEBO in the figure (well-known hysteresis behavior). As we traverse along the different segments of the bifurcation diagram, the ignition behavior changes. There is no ignition in the segment OI. As we move from A to C, the ignition behavior changes from back-end to front-end. (Note: For very high values of inlet fluid temperature, front-end ignition is favored.) In the segment CE (as we traverse from C to E), the ignition behavior changes from front-end to back-end. Close to the extinction point, it is a back-end ignition. Similar behavior will be obtained for the case where washcoat diffusion is included.

## Discussion and Conclusions

The main contribution of this work is the presentation of an analytical light-off criterion for general kinetics in a monolith and elucidation of the ignition behavior with changes in feed temperature. The result of this work can be combined with the earlier analysis of Ramanathan et al.[12] to obtain optimal design of catalytic converters to minimize cold-start emissions. Reducing the ignition temperature by >30 K would decrease the transient time required for ignition. Also, favoring front-end ignition would help achieve the maximum possible conversion

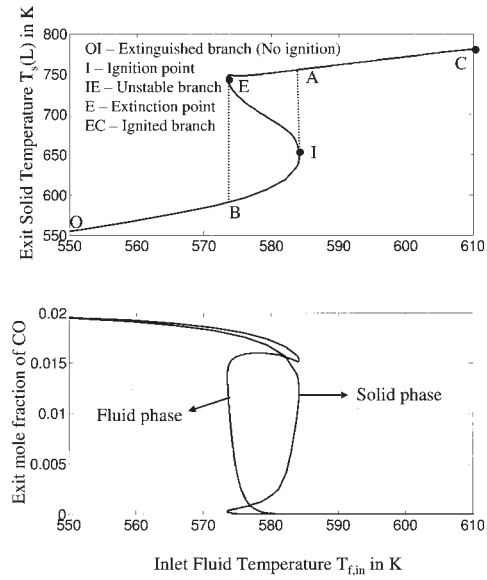


**Figure 5. Bifurcation diagrams of exit monolith temperature vs. inlet fluid temperature for parameter values listed in Table 1.**

(because the entire monolith would be ignited) apart from reducing the transient time (compared to back-end ignition). The analytical ignition criterion can be used in other applications to find designs that favor front-end or back-end ignition.

It would be interesting to compare the light-off criterion presented here to experimental light-off data on CO oxidation. Unfortunately, there are no systematic studies in the literature that show how the light-off temperature (or location) varies with catalyst loading, catalyst axial distribution, monolith dimensions, inlet concentration of CO, and thermal conductivity of the support. However, the general trends such as the increase in light-off temperature with increasing inlet CO concentration (negative order kinetic effect) and decrease in the light-off temperature with increased Pt/Pd loading have been verified.

## Acknowledgments

This work was supported by grants from the Robert A. Welch Foundation and The Dow Chemical Company.

## Notation

$a_c(x)$ = catalyst distribution function along the channel length
$C$ = concentration, mol/m$^3$
$C_{m,in}$ = inlet fluid concentration
$D_e$ = effective diffusivity of reactant in the washcoat
$D_m$ = diffusion coefficient in the fluid phase
$E$ = activation energy
$h(x)$ = position-dependent heat-transfer coefficient
$k_c(x)$ = position-dependent mass-transfer coefficient
$k_f$ = fluid thermal conductivity
$k_w$ = solid thermal conductivity
$L$ = length of the monolith channel
$M_w$ = molecular weight
Nu = Nusselt number
P = transverse Peclet number ($=R_\Omega^2\bar{u}/LD_m$)
$Pe_h$ = heat Peclet number
$R_g$ = universal gas constant
$R_\Omega$ = channel hydraulic radius
Sh = Sherwood number
$T$ = fluid temperature
$T_{f,in}$ = inlet fluid temperature
$\bar{u}$ = average fluid velocity in the channel
$x$ = coordinate along the length of the channel
$y$ = mole fraction or transverse coordinate

### Greek letters

$\delta_c$ = effective thickness of the washcoat
$\delta_w$ = effective wall thickness
$\eta$ = effectiveness factor

### Subscripts and superscripts

$f$ = fluid phase and/or cup-mixing
$m$ = cup-mixing
$s$ = solid phase

## Literature Cited

1. Cybulski A, Moulijn JA. Monoliths in heterogeneous catalysis. *Catal Rev Sci Eng.* 1994;36:179-270.
2. Lox ESJ, Engler BH. Environmental catalysis, In: Ertl G, Weitkam J, Knozinger H, eds. *Handbook of Heterogeneous Catalysis*. Vol. 4. New York, NY: Wiley; 1997:1559-1631.
3. Groppi G, Belloli A, Tronconi E, Forzatti P. A comparison of lumped and distributed models of monolithic catalytic combustors. *Chem Eng Sci.* 1995;50:2705-2715.
4. Becker EG, Pereira CJ, eds. *Computer Aided Design of Catalysts*. New York, NY: Marcel Dekker; 1993.
5. Hayes RE, Kolaczkowski ST. *Introduction to Catalytic Combustion*. Amsterdam, The Netherlands: Gordon & Breach Science Publishers; 1997.
6. Please CP, Hagan PS, Schwendeman DW. Light-off behavior of catalytic converters. *SIAM J Appl Math.* 1994;54:72-92.
7. Leighton DT, Chang H-C. A theory for fast-igniting catalytic converters. *AIChE J.* 1995;41:1898-1915.
8. Keith JM, Chang H-C, Leighton DT. Designing a fast-igniting catalytic converter. *AIChE J.* 2001;47:650-663.
9. Oh SH, Cavendish JC. Mathematical modeling of catalytic converter lightoff. Part III: Prediction of vehicle exhaust emissions and parametric analysis. *AIChE J.* 1985;31:943-949.
10. Ramanathan K, Balakotaiah V, West DH. Light-off criterion and transient analysis of catalytic monoliths. *Chem Eng Sci.* 2003a;58:1381-1405.
11. Ramanathan K, Balakotaiah V, West DH. Bifurcation analysis of catalytic monoliths with nonuniform catalyst loading. *Ind Eng Chem Res.* 2003b;43:288-303.
12. Ramanathan K, West DH, Balakotaiah V. Optimal design of catalytic converters for minimizing cold-start emissions. *Catal Today.* 2004c;98:357-373.
13. Balakotaiah V. Simple runaway criteria for cooled reactors. *AIChE J.* 1989;35:1039-1043.
14. Voltz SE, Morgan CR, Liederman D, Jacob SM. Kinetic study of carbon monoxide and propylene oxidation on platinum catalysis. *Ind Eng Chem Prod Res Dev.* 1973;12:294-301.

*Manuscript received Jun. 15, 2005, and revision received Nov. 4, 2005.*